Contents lists available at ScienceDirect

Phytomedicine

Original Article

Zingiberene, a non-zinc-binding class I HDAC inhibitor: A novel strategy for the management of neuropathic pain

Vittoria Borgonetti [a,1], Paolo Governa [b,1], Fabrizio Manetti [b], Nicoletta Galeotti [a,*]

[a] Department of Neuroscience Psychology, Drug Research and Child Health (NEUROFARBA), Section of Pharmacology, University of Florence, Viale G. Pieraccini 6, I-50139, Florence, Italy
[b] Department of Biotechnology Chemistry and Pharmacy, Department of Excellence 2018-2022, University of Siena, via Aldo Moro 2, I-53100, Siena, Italy

A R T I C L E   I N F O

A B S T R A C T

Background: Even though numerous Histone deacetylase inhibitors (HDACi) have been approved for the treatment of different types of cancer, and others are in clinical trials for the treatment of neurodegenerative diseases, the main problem related to the clinical use of available HDACi is their low isoform selectivity which causes undesirable effects and inevitably limits their therapeutic application. Previously, we demonstrated that a standardized *Zingiber officinalis* Roscoe rhizome extract (ZOE) reduced neuroinflammation through HDAC1 inhibition in a mice model of neuropathy, and this activity was related to terpenes fraction.
Hypothesis/Purpose: The aim of this work was to identify the ZOE constituent responsible for the activity on HDAC1 and to study its possible application in trauma-induced neuropathic pain.
Methods: The ability of ZOE and its terpenes fraction (ZTE) to inhibit HDAC and SIRT isoforms activity and protein expression was assessed *in vitro*. Then, a structure-based virtual screening approach was applied to predict which constituent could be responsible for the activity. In the next step, the activity of selected compound was tested in an *in vitro* model of neuroinflammation and in an *in vivo* model of peripheral neuropathy (SNI).
Results: ZTE resulted to be more potent than ZOE on HDAC1, 2, and 6 isoforms, while ZOE was more active on HDAC8. Zingiberene (ZNG) was found to be the most promising HDAC1 inhibitor, with an IC_{50} of 2.3 ± 0.1 μM. A non-zinc-binding mechanism of inhibition was proposed based on molecular docking. Moreover, the oral administration of ZNG reduced thermal hyperalgesia and mechanical allodynia in animals with neuropathy after 60 min from administration, and decreased HDAC-1 levels in the spinal cord microglia.
Conclusion: We found a new non-zinc-dependent inhibitor of HDAC class I, with a therapeutic application in trauma-related neuropathic pain forms in which microglia-spinal overexpression of HDAC1 occurs. The non-zinc-binding mechanism has the potential to reduce off target effects, leading to a higher selectivity and better safety profile, compared to other HDAC inhibitors.

Introduction

Neuroinflammation has been reported as one of the key points in the pathogenesis of various pathological states affecting the central nervous system (CNS), including: neurodegenerative diseases, chronic pain, anxiety, and depression (Kwon et al., 2020). The pivotal role of microglial cells in the induction, maintenance, and development of the inflammatory processes and how these can drastically affect the conditions of the surrounding environment have been deepened by recent scientific literature (Chuang et al., 2016; Marinelli et al., 2019; Subhramanyam et al., 2019). In fact, the functional and morphological changes of the branched microglia in the activated phenotype led to the production of inflammatory factors capable of damaging normal neuronal activity, which results in altered physiological functions (O'Loughlin et al., 2018).The scientific interest in finding new possible targets capable of inhibiting the microglial activation process is, consequently, growing. Epigenetics influence on the modulation of microglial activity and the protective activity towards the neuroinflammation process of some histone deacetylase inhibitors (HDACi) has been postulated (Garden, 2013). Recently, it has been demonstrated that the inhibition of HDAC1 leads to a significant reduction in the activation of NF-κBp65, a well-known marker of microglial activation (Romanelli et al., 2021), highlighting an important role for the HDAC1 isoform.

Even though numerous HDACi have been approved by the Food and Drug Administration (FDA) for the treatment of different types of cancer, and others are in clinical trials for the treatment of neurodegenerative diseases (Hontecillas-Prieto et al., 2020; Valente et al., 2014), the main problem related to the clinical use of available HDACi is their low isoform selectivity which causes undesirable effects and inevitably limits their therapeutic application (Gao et al., 2019). For this reason, the search for new possible active ingredients with activity towards specific HDAC isoforms to selectively address pathological conditions, is of great interest. Previously, we demonstrated that a standardized *Zingiber officinalis* Roscoe rhizome extract (ZOE) reduced neuroinflammation through HDAC-1 inhibition in a mice model of neuropathy, and this activity was related to terpenes fraction (Borgonetti et al., 2020). In this work, molecular docking approaches were applied to predict which terpene compound isolated from ZOE could be responsible for the inhibition of the HDAC1 activity. In the next step, the evaluation of the inhibitory activity in an *in vitro* model of neuroinflammation and the efficacy in an *in vivo* model of peripheral neuropathy was also performed to assess the potential clinical relevance of such a compound.

Material and methods

Chemicals

ZOE, a supercritical CO_2 extract, standardized to contain 24.73% total gingerols and 3.03% total shogaols, was kindly provided by INDENA S.p.A. (Milan, Italy), batch number 46,349. ZOE terpenes fraction (ZTE) was extracted from ZOE as previously reported (Borgonetti et al., 2020). The HPLC-DAD and GC–MS chemical characterization of ZOE and ZTE is also described in our previous paper (Borgonetti et al., 2020). Zingiberene (ZNG, purity > 98%) was purchased from Santa Cruz Biotechnology (Santa Cruz, CA). Bacterial lipopolysaccharide (LPS) from Gram- (*Salmonella enteridis*) was purchased from Sigma-Aldrich (Milan, Italy).

Cell culture

A murine microglial line BV-2 (mouse, C57BL / 6, brain, microglial cells, Tema Ricerca, Genova, Italy) was used for this study. The cells were thawed and cultured in 75 cm^2 flasks (Sarstedt, Milan) in RPMI medium, containing 10% heat-inactivated (56 °C, 30 min) fetal bovine serum (FBS, Gibco®, Milan) and 1% glutamine. Cells were grown at 37 °C and 5% CO_2 with daily medium change (Borgonetti et al., 2020).

Cells treatments and neuroinflammation model

Microglial cells (3×10^5 cells/well) were seeded in 6-well plates until 70–80% confluence was achieved. The cells were then pretreated with ZOE (10 μg ml^{-1}), ZTE (3 μg ml^{-1}), and suberoylanilide hydroxamic acid (SAHA, 5 μM) for 4 h and then stimulated with LPS, (250 ng ml^{-1}) for 24 h. The substances were dissolved in ethanol 96% V/V.

HDAC and sirtuin (SIRT) isoforms activity assay

The effects of ZOE and ZTE on the enzymatic activities of recombinant human HDAC1, 2, 3, 4, 5, 6, 7, 8, 9, 11, SIRT1, 2, 3, 5, and 6 was determined using an *in vitro* enzymatic assay (BPS Bioscience, San Diego, CA), following the instruction provided by the vendor. SAHA (Cayman chemical, Ann Arbor, MI), trichostatin A (Selleck, Huston, TX), suramin (Cayman chemical), and nicotinamide (Sigma-Aldrich) were used as reference compounds for HDAC1, 2, 3, 6, HDAC4, 5, 7, 8, 9, 11, SIRT1, and SIRT2, 3, 5, 6, respectively. ZOE, ZTE, and reference compounds were tested at the single concentration of 5 μg ml^{-1}, 1.6 μg ml^{-1}, and 0.01 μM, respectively. A full dose-response curve (11 points) was performed in triplicate for ZNG on HDAC1.

Animals

CD1 male mice, weighing 20–22 g, were obtained from Envigo (Varese, Italy) and housed in standard cages with 4–5 animals per cage. The cages were placed in the experimental room for acclimatization 24 h before behavioral testing. The mice were provided with standard laboratory food and water *ad libitum* and kept under controlled conditions of temperature (23 °C) and a 12-hour light/dark cycle (light on at 7:00 AM). All animal care and experimental protocols were in compliance with international laws and policies, including Directive 2010/63/EU of the European parliament and of the council of 22 September 2010 on the protection of animals used for scientific purposes and the Guide for the Care and Use of Laboratory Animals, US National Research Council, 2011. The protocols were also approved by the Animal Care and Research Ethics Committee of the University of Florence, Italy, under license from the Italian Department of Health (54/2014-B, 410/2017-PR 12/5/2017) and in accordance with the animal research: reporting of *in vivo* experiments (ARRIVE) guidelines (du Sert et al., 2020; Lilley et al., 2020). The number of animals used in each experiment was determined using a power analysis with G power software (Charan et al., 2013), and all efforts were made to minimize animal suffering. A total of 8 animals were included in each tested group for the evaluation of anti-nociceptive effects. Mice were euthanized by cervical dislocation for the removal of spinal cord tissue for *in vitro* analysis.

Spared nerve injury (SNI) model

As previously reported (Borgonetti et al., 2021a), mice were anesthetized using a mixture of 4% isoflurane in O2/N2O (30:70 V/V) and positioned in a prone position. The right hind limb was slightly elevated and a skin incision was made on the lateral surface of the thigh. The sciatic nerve was exposed and both the tibial and common peroneal nerves were secured with a microsurgical forceps (5.0 silk, Ethicon; Johnson & Johnson Intl, Brussels, Belgium) and cut together. The uninjured sural extensions were used to assess the mechanical allodynia and thermal hyperalgesia associated with the model. The sham procedure involved the same surgery without ligation and severing of the nerves.

Drug administration

To ensure unbiased group assignment, mice were randomly assigned

to each group by an individual other than the operator. ZNG was dissolved in 1% sodium carboxymethyl cellulose and administered via gavage before testing at a dose of 10 mg/kg, which is the concentration present in the active dose of ZOE (200 mg/kg). Pregabalin (30 mg/kg), a reference drug, was dissolved in saline and administered intraperitoneally 3 h before testing. LG325, a selective HDAC1 inhibitor synthesized in the laboratory of Professor Maria Novella Romanelli at the University of Florence, Italy, was administered by intrathecal injection at a dose of 5 µg per mouse 15 min before testing, as previously described (Borgonetti et al., 2021a).

Behavioural tests

Behavioural tests were performed before surgery, to establish a baseline for comparison with postsurgical values, and 10 days after surgery by a blinded operator.

Hot plate test

The hot plate test involves the evaluation of thermal hyperalgesia using a circular metal surface (24 cm diameter) electrically heated to a temperature of about 52.5 °C. The mice are placed on the hot plate surrounded by a transparent acrylic cage and the response time of the animals to the hyperalgesic stimulus is measured. Response latency (measured in s) consists of a leap, licking, or shaking of the paw. The mouse is immediately removed from the plate when it exhibits any of these symptoms. The animals were tested one at a time and did not undergo a period of adaptation to the experimental system prior to testing (Borgonetti et al., 2021a).

Von Frey filaments

The Von Frey test was used to evaluate mechanical allodynia (Borgonetti et al., 2020). The tests were carried out both before the operations, using the data obtained as a reference, and afterwards for comparison. Mechanical nociception was measured by Von Frey monofilaments. Mice were placed in single plexiglass chambers [8.5 × 3.4 × 3.4 (h) cm]. After a settling period of 1 h inside the chambers, the mechanical threshold was measured through a stimulus using Von Frey monofilaments with increasing degree of strength (0.04, 0.07, 0.16, 0.4, 0.6, 1.0, 1.4, 2.0 g) on both legs, ipsilateral and contralateral. The response was defined by the withdrawal of the paw three times out of five stimuli performed. In the event of a negative response, the next higher-grade strand was applied, and the averages of the responses were finally calculated.

Immunofluorescence

On day 7, the animals were perfused transcardially with 4% paraformaldehyde in 0.1 M phosphate buffered saline (PBS, pH 7.4). After perfusion, the lumbar spinal cord was promptly removed, postfixed for 18 h with the same fixative at 4 °C, and transferred to solutions of decreasing concentrations of sucrose (10%, then 20%, and finally 30%). After preincubation in a solution of 5 mg/ml bovine serum albumin (BSA)/0.3% Triton-X-100/PBS, sections were incubated overnight at 4 °C with primary antibodies at optimized working dilutions. The primary antibodies used were those specific for glial fibrillary acidic protein HDAC1 (1:100; Santa Cruz Biotechnology) and integrin alpha-M (CD11b) (1:100; Bioss Antibodies). After rinsing in PBS containing 0.01% Triton-X-100, the sections were incubated with secondary antibodies labeled with Invitrogen Alexa Fluor 488 (490–525, 1:400; Thermo Fisher Scientific), Invitrogen Alexa Fluor 568 (578–603, 1:400; Thermo Fisher Scientific), and Cruz Fluor 594 (592–614, 1:400; Santa Cruz Biotechnology) at rt for 2 h. The sections were then mounted with Vectorshield mounting medium (Vector Laboratories, Burlingame, CA) and analyzed using a Leica DM6000B fluorescence microscope equipped

with a DFC350FX digital camera and appropriate excitation and emission filters for each fluorophore. Representative images were acquired with objectives ranging from 5X to 40X, and the immunofluorescence intensity was calculated using Image J software (Wayne Rasband, National Institute of Health, USA) (Borgonetti et al., 2020).

Preparation of tissue and cell lysates

Proteins extraction from tissues and cells were performed as previously observed (Borgonetti et al., 2021b). Briefly, proteins from BV2 cells were extracted by radioimmunoprecipitation assay buffer (RIPA) buffer (50 mM Tris–HCl pH 7.4, 150 mM NaCl 1% sodium deoxycolate, 1% Tryton X-100, 2 mM PMSF) (Sigma-Aldrich) and the insoluble pellet was separated by centrifugation (12,000 × g for 30 min, 4 °C). The total protein concentration in the supernatant was measured using Bradford colorimetric method (Sigma-Aldrich). To examine protein expression, mice were sacrificed, and the lumbar spinal cord tissue was removed 10 days after surgery. Samples were homogenized in a lysis buffer containing 25 mM Tris–HCl pH 7.5, 25 mM NaCl, 5 mM ethylene glycol tetraacetic acid (EGTA), 2.5 mM ethylenediaminetetraacetic acid (EDTA), 2 mM NaPP, 4 mM p-nitrophenylphosphate (PNFF), 1 mM di Na_3VO_4, 1 mM phenylmethylsulfonyl fluoride (PMSF), 20 µg ml^{-1} leupeptin, 50 µg ml^{-1} aprotinin, 0.1% SDS (Sigma-Aldrich). The homogenate was centrifuged at 12,000 × g for 30 min at 4 °C and the pellet was discarded.

Western blotting

Protein samples (40 µg of protein/sample) were separated by 10% SDSPAGE (Borgonetti et al., 2021b). Proteins were then blotted onto nitrocellulose membranes (120 min at 100 V) using standard procedures. Membranes were blocked in PBS with 1% tween 20 (PBST) containing 5% non-fat dry milk for 120 min and incubated overnight at 4 °C with primary antibodies HDAC1 (1:1000), HDAC2 (1:1000), HDCA3 (1:1000), HDAC4 (1:1000), HDAC5 (1:1000), HDAC6 (1:1000), HDAC8 (1:1000), HDAC11 (1:1000), SIRT1 (1:1000), anti-IKBα (1:1000, sc-1643) (Santa Cruz Biotechnology), anti-IL-1β (1:1000, bs6319R) (Bioss Antibodies, MA, USA). The blots were rinsed three times with PBST and incubated for 2 h at rt with HRP-conjugated mouse anti-rabbit (1:3000, sc-2357) (Santa Cruz Biotechnology) and goat anti-mouse (1:5000, bs-0296 G,) (Bioss Antibodies) and then detected by chemiluminescence detection system (Pierce, Milan, Italy). Signal intensity (pixels/mm^2) was quantified using ImageJ (NIH). The signal intensity was normalized to that of GAPDH (1:5000, sc-32,233) (Santa Cruz Biotechnology).

Molecular docking

All ligands were drawn with Maestro (release 2021–3) and minimized with the LigPrep routine (OPLS3e force field), while ionization and tautomeric states were generated at pH ranging from 6.0 to 8.0 by Epik software. A Systematic Pseudo Monte Carlo conformational search was then applied to generate 200 conformations for each compound.

Molecular docking simulations were performed using AutoDock Vina (Forli et al., 2016) . Briefly, the X-ray structure of human HDAC2 in complex with SAHA was retrieved from the RCSB Protein Data Bank (PDB ID: 4LXZ). All water molecules and ions were removed using PyMol (The PyMOL Molecular Graphics System, Version 2.0 Schrödinger, LLC) and AutoDock Tools (Morris et al., 2009) was used to prepare ligands and protein for docking simulations. The grid box was centered on the ligand and set to 24 × 18 × 18 points in x, y, z dimension, respectively, with default 1 Å spacing. The exhaustiveness was set to 24.

The co-crystalized ligand was re-docked to validate the reliability of the docking program.

Table 1
Inhibitory activity of ZOE, ZTE, and reference compounds on HDAC and SIRT isoforms activity.

Enzyme	% inhibition ± SD		
	ZOE (5 μg ml^{-1})	ZTE (1.6 μg ml^{-1})	Reference compound
HDAC1	4.5 ± 0.5	9.0 ± 2.0	19.5 ± 0.5*
HDAC2	2.5 ± 0.5	8.5 ± 2.5	14 ± 0.5*
HDAC3	9.5 ± 0.5	9.5 ± 0.5	21 ± 0.5*
HDAC4	2.5 ± 0.5	2.0 ± 0.5	15 ± 0.5°
HDAC5	1.5 ± 1.5	0.5 ± 0.5	29.5 ± 0.5°
HDAC6	0.5 ± 0.5	3.5 ± 0.5	6.0 ± 0.5*
HDAC7	5.0 ± 0.5	4.0 ± 0.5	9.5 ± 0.5°
HDAC8	7.5 ± 0.5	3.0 ± 1.0	11.0 ± 1.0°
HDAC9	2.0 ± 0.5	0.5 ± 0.5	29.5 ± 0.5°
HDAC11	1.0 ± 0.5	0.5 ± 0.5	10.0 ± 0.5°
SIRT1	2.0 ± 0.5	1.0 ± 0.5	11.01 ± 1.0#
SIRT2	0.5 ± 0.5	1.5 ± 0.5	10.0 ± 2.0^
SIRT3	1.5 ± 0.5	3.5 ± 0.5	11.0 ± 0.5^
SIRT5	1.5 ± 0.5	0.5 ± 0.5	17.5 ± 0.5^
SIRT6	2.5 ± 0.5	3.0 ± 0.5	18.5 ± 1.5^

*SAHA, 0.01 μM; ° trichostatin A, 0.01 μM; # suramin, 0.01 μM; ^ nicotinamide, 0.01 μM.

Statistical analysis

The data and statistical analysis in this study adhere to the recommendations for experimental design and analysis in pharmacology (Curtis et al., 2018). For *in vitro* analysis, data are expressed as the mean ± SEM of five experiments and analyzed using one-way and two-way ANOVA followed by Tukey post hoc testing. Behavioral data are presented as means ± SEM and analyzed using two-way ANOVA followed by Bonferroni post hoc testing. A total of 8 animals were used in the VEH SNI, PREG, and LG325 groups, and 13 animals were used in the ZNG group. The unpaired sample *t*-test was used for analysis of locomotor activity. Statistical analyses were performed using GraphPad Prism version 5.0 (GraphPad Software, San Diego, CA), and a *p*-value of <0.05 was considered significant.

Results

ZTE fraction selectively reduced the HDAC1, HDAC2, HDAC3, HDAC8, and HDAC11 activity and protein expression in LPS-stimulated BV2.

Previous results showed that ZTE might represent the fraction mainly involved in the modulation of HDAC1 activity (Borgonetti et al., 2020). To verify the capability of ZOE and ZTE to inhibit HDAC activity, we performed an enzymatic assay. The percentage of inhibition of ZOE, ZTE, and positive control on HDAC1–9 and −11, SIRT1–3, and SIRT5–6 are reported in Table 1. Although the values of percentage of inhibition were low, ZOE demonstrated a higher inhibitory activity on HDAC3 and

8, compared to the other isoforms, while ZTE on HDAC1, 2, and 3. No effect was observed on the modulation of sirtuins. ZTE was found to be more potent than ZOE on HDAC1, 2, and 6 isoforms, while ZOE was more active on HDAC8. No activity was observed on sirtuins.

The stimulation with LPS for 24 h has been demonstrated to cause morphological and phenotype changes in BV2 leading cells to shift toward a proinflammatory microglia phenotype (Borgonetti et al., 2020). In this condition, we observed that HDAC1, 2, 3, and 8 (*i.e.*, class I HDACs) and HDAC11 (class IV) were up regulated, while no effect was produced in HDAC4, 5, 6 (class II), and SIRT (class III). A significant reduction in HDAC6 levels was observed in microglial cells following inflammatory stimulation (Fig. 1A).

As reported in Fig. 1B, HDAC isoforms 1, 2, 3, 8, and 11 appear to be increased in LPS-stimulated BV2 cells. ZOE (10 μg/ml) reduced the expression of HDAC1, 2, 8, and 11, with an efficacy comparable to that of SAHA, a known HDAC pan-inhibitor (Borgonetti et al., 2021a), used as positive control. No effect was observed on the expression of HDAC3. ZTE (3 μg/ml), tested at the concentration present in the active dose of ZOE, showed an efficacy comparable to ZOE on the expression of HDAC1 and HDAC11. A reduction of the protein levels of HDAC2 and HDAC8, compared to LPS-stimulated BV2 was also observed, even if with a lower efficacy, compared to ZOE.
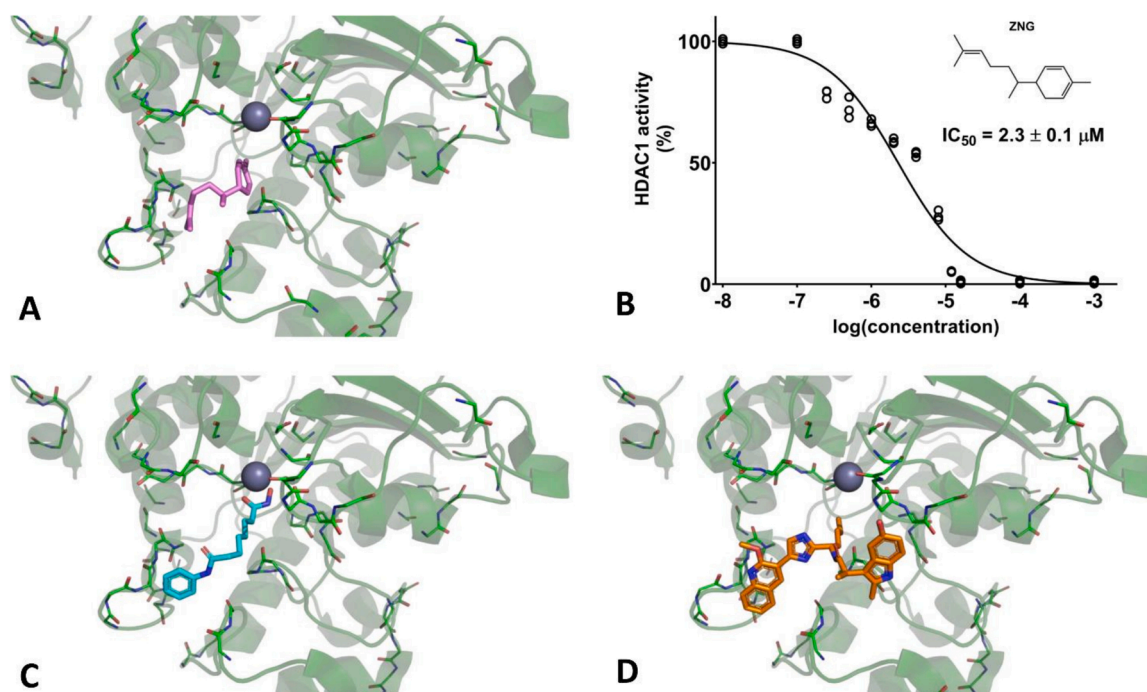
In silico and in vitro HDAC1 inhibitory activity of ZNG

Previous results showed the capability of ZOE to reduce HDAC1 overexpression in neuropathies (Borgonetti et al., 2020). Furthermore, a selective overexpression of HDAC1 and 2 was observed in spinal cord samples of SNI mice (Fig. 1B). Given this selectivity, we performed molecular docking simulations to identify which ZTE constituent could be responsible for HDAC1 inhibition. As the crystal structure of HDAC1 in complex with an inhibitor is not currently available, we used the crystal structure of HDAC2, which share high sequence identity (85.06%) with HDAC1, in complex with SAHA (also referred to as vorinostat), as a target. Among the 35 volatile constituents identified in ZOE by GC–MS, ZNG, the most abundant compound, was found to have a better binding affinity compared to other constituents, with a Vina binding energy of −7.1 kcal/mol. Moreover, its lipophilic nature matches the hydrophobic nature of HDAC2 binding site, allowing the establishment of van der Waals contacts with His33, Pro34, Asp104, Gly154, Phe155, His183, Phe210, Leu276, and Tyr308 (Fig. 2A). Except from Tyr308, all these interactions are also established by SAHA, used as a reference compound (Fig. 2C). Differently from SAHA, which possess a zinc-binding group, ZNG cannot coordinate the zinc ion present in the binding site of HDAC1. However, non-zinc-binding HDACi of natural origin, such as ursolic acid, epicocconigrones, curcumin, *n*-butyric acid, and aceroside VIII, are already known (Akone et al., 2020). Moreover, a small library of non-zinc-binding HDACi, based on the structure of the
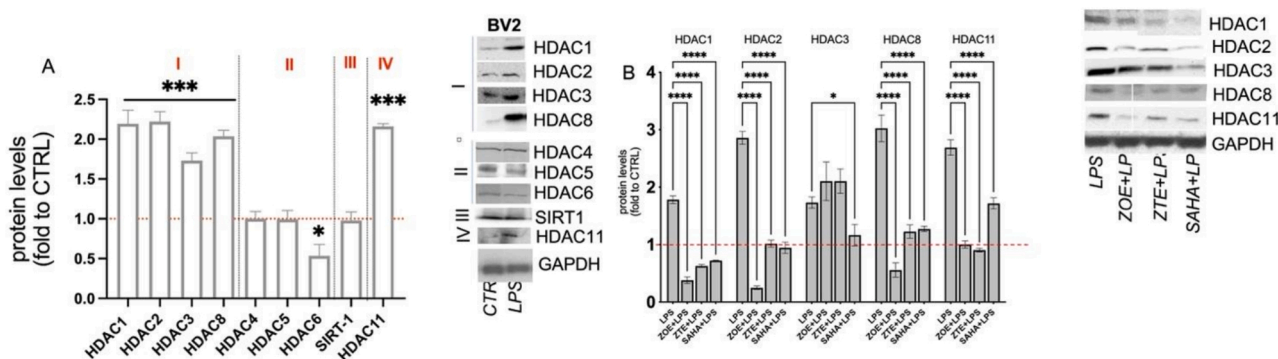
**Fig. 1.** A) HDACs isoforms expression in LPS-stimulated BV2 (250 ng ml^{-1}) for 24 h, compared to untreated microglia cells (red dashed line; One-way ANOVA ***p<0.001 *p<0.5). Effects produced by ZOE (10 μg/ml) and ZTE (3 μg/ml) pretreatment on HDAC1, 2, 3, 8 and 11 in LPS-stimulated BV2 (250 ng ml^{-1}) for 24 h, compared to untreated microglia cells (red dashed line; One-way ANOVA ****p<0.0001; *p<0.5).

Fig. 2. A) Docking pose of zingiberene (ZNG, violet) in the binding site of HDAC2. B) *In vitro* HDAC1 inhibitory activity of ZNG. For comparison to the experimental binding mode of (C) SAHA (cyan), PDBID: 4LXZ, and (D) non-zinc-binding HDAC1, 2, 3, 10, and 11 inhibitor (compound 19, orange), PDBID:7LTL are shown.
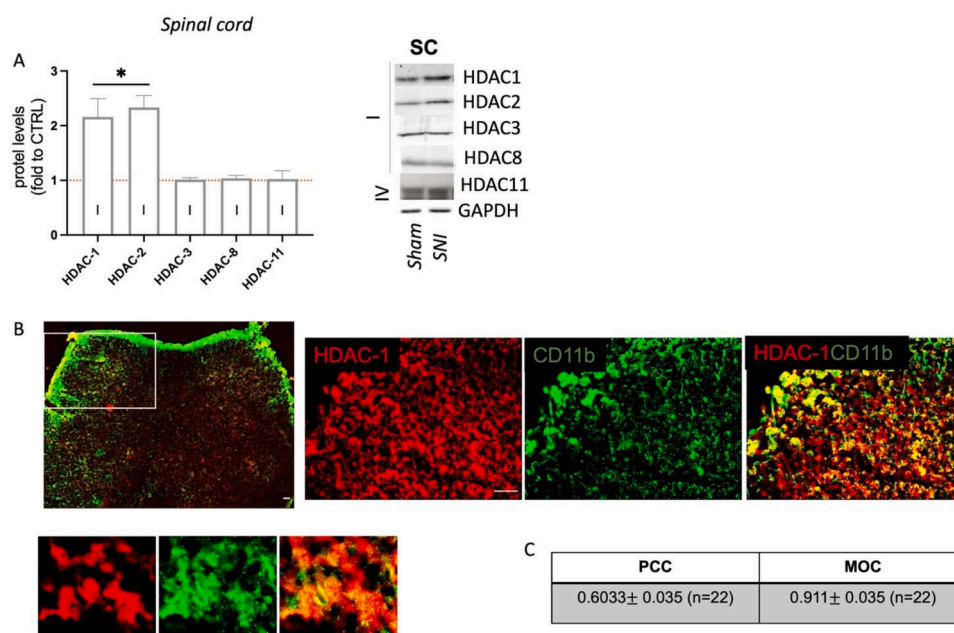

Fig. 3. A) Expression of HDAC1, 2, 3, 8, and 11 in spinal cord tissue of animal with neuropathy compared to the sham group (red dashed line; One-way ANOVA *p<0.05). B) Representative colocalization images of HDAC1 (red) and CD11b (green) in the spinal cord tissue of SNI mice with different magnification: 5x and 20x (scale bar 50 μm). C) Quantification of Pearson's coefficient (PCC) and Mander's coefficient (MOC). Representative blots are also showed.

natural product apicidin, have been reported, with the advantages of not containing electrophilic substructures, thus reducing the risk of off-target effects, and of being negative in the Ames mutagenicity assay, while still having high potency and cellular activity comparable to clinically used HDACi (Beshore et al., 2021). Indeed, the docking pose of ZNG is very similar to the binding mode of the HDAC1, 2, 3, 10, and 11 selective inhibitor (reported as compound 19) observed in the crystal structure (PDBID: 7LTL; Fig. 2D), and maintains hydrophobic contacts with Phe155 and Phe210, which are crucial for the binding of compound

19. To confirm the docking results, we evaluated the inhibitory activity of ZNG on HDAC1 *in vitro*, using an enzymatic assay. ZNG showed an IC_{50} of 2.3 μM (Fig. 2B).

HDAC class I and IV are expressed in ipsilateral side of SNI mice spinal cord

To validate the LPS-stimulated BV2 model as predictive for the evaluation of HDAC activity in a neuroinflammation-based pathological
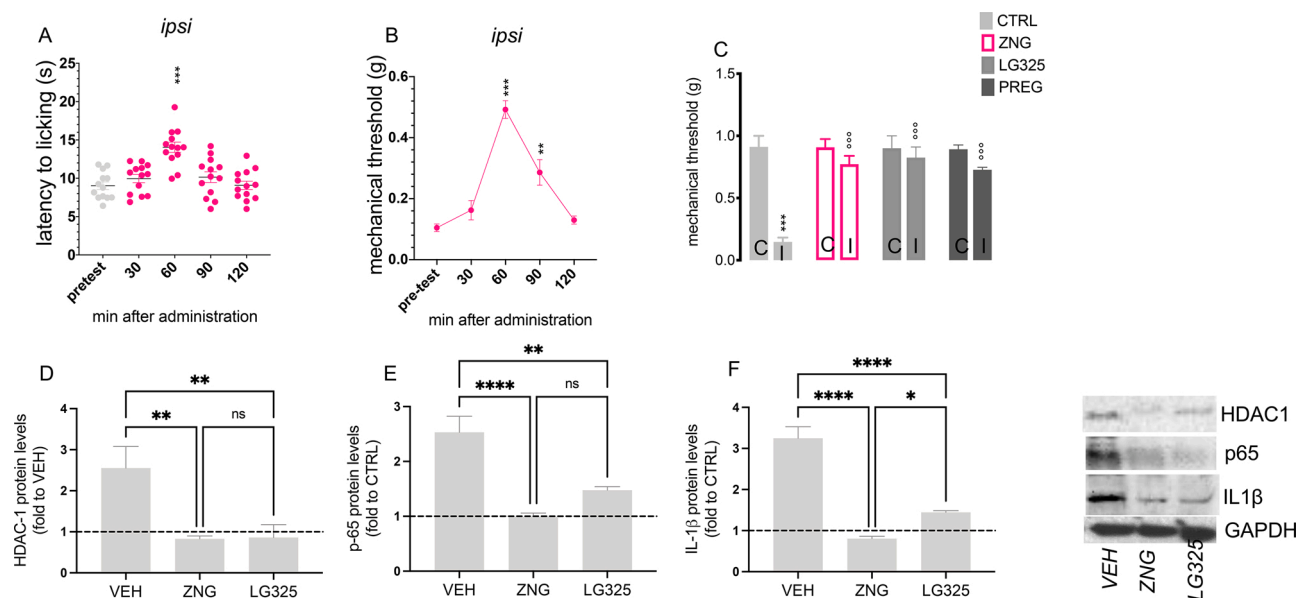
Fig. 4. Effects of ZNG on thermal hyperalgesia measured with hot plate test (A) and mechanical allodynia measured with Von Frey filaments after 30, 60, 90, and 10 min from oral administration in SNI mice. (Two-way ANOVA ***$p<0.001$ **$p<0.01$). Comparison of the effect obtained with ZNG, LG325, and PREG on mechanical allodynia produced by the SNI model (Two-way ANOVA ***$p<0.001$ vs CTRL contra, °°°$p<0.001$ vs CTRL ipsi). HDAC1 (D), p-65 (E), and IL-1β (F) protein expression on ipsilateral side of SNI mice spinal cord compared the contralateral side (black dashed line). (One-way ANOVA ****$p<0.0001$, **$p<0.01$, *$p<0.05$). Representative blots are also showed.

condition, we detected the HDAC class I and IV expression in the spinal cord of SNI mice. In the SNI model, animals with neuropathy showed an increase in HDAC1 and HDAC2 expression in the spinal cord, compared to control, while no effect was observed regarding the expression of HDAC3, 8, and 11 (Fig. 3A). As previously observed (Borgonetti et al., 2022, 2021a), Fig. 3B shows the colocalization of HDAC1 with CD11b, a marker of pro-inflammatory phenotype microglia, thus suggesting the activation of HDAC1 and HDAC2 as targets in microglial activation in the spinal cord of animals with neuropathy.

ZNG reduces HDAC1 protein expression in spinal cord of SNI mice and reduced neuropathic pain symptoms

HDAC1 inhibitors have shown activity in reducing symptoms associated with neuropathic pain (Romanelli et al., 2021). To investigate whether the inhibitory activity of ZNG on HDAC1 activity observed *in vitro* may have an effect in reducing symptoms associated with neuropathic pain, we treated SNI animals with 20 mg/kg ZNG. The oral administration of ZNG reduced thermal hyperalgesia (Fig. 4A) and mechanical allodynia (Fig. 4B) in animals with neuropathy after 60 min from administration. We also compared the effect of ZNG on mechanical allodynia with that produced by LG325, a selective HDAC1 inhibitor (Sanna et al., 2017), and pregabalin (PREG), used as reference drug in neuropathic pain. ZNG produced a similar effect, compared to the positive controls (Fig. 4C). In the spinal cords of neuropathic animals, we observed an increase in the expression of HDAC1, which was completely reverted by ZNG, similarly to animals treated with SAHA (Fig. 4D). HDAC1 can increase the expression of factors related to inflammation and microglial activation (Borgonetti et al., 2021a). For this reason, we evaluated the effect of ZNG and SAHA on the expression of NF-κBp65. In SNI animals, we observed an increase in the expression of this transcription factor, which was completely counteracted by ZNG and SAHA (Fig. 4E). The activation of NF-κBp65 induces an increase in the expression of pro-inflammatory cytokines. IL-1β is one of the major pro-inflammatory cytokines produced by microglia and is up-regulated in the spinal cord of animals with neuropathy (Borgonetti et al., 2020). Consistently, SNI mice showed an increase in the expression of this protein, with ZNG and SAHA reducing this effect to values like the

unoperated control (dashed line).

Discussion

Neuroinflammation has been widely demonstrated to be one of the key points in the pathogenesis of various CNS pathological states, including neurodegenerative diseases, chronic pain, anxiety, and depression (Finnerup et al., 2020). The central role of microglial cells in the induction, maintenance, and development of the inflammatory process, and how they can dramatically affect the conditions of the surrounding environment have been deeply explored in recent scientific literature (Block et al., 2007; Marinelli et al., 2019; Subhramanyam et al., 2019; Szepesi et al., 2018). Indeed, the functional and morphological change of the branched microglia in an activated phenotype leads to the production of inflammatory factors capable of damaging normal neuronal activity, altering its physiological functions (Marinelli et al., 2019). The scientific interest in finding new possible targets capable of inhibiting the microglial activation process is therefore growing. It has recently been shown that epigenetics can influence the modulation of microglial activity and that certain HDACi have been shown to have protective activity against the process of neuroinflammation (Ellis et al., 2013; Garden, 2013). Several HDACi have been approved by the FDA for the treatment of certain types of cancer, and others are in clinical trials for the treatment of neurodegenerative diseases (Bondarev et al., 2021). The main problem with the clinical use of pan-HDACi is their low specificity, which causes undesirable effects and inevitably limits their therapeutic application. Therefore, the search for possible new active principles with selective activity towards specific HDAC isoforms expressed in certain pathological conditions is of great interest. For this reason, we have deepened the possible effects induced by a standardized *Zingiber officinale* Roscoe extract (ZOE) and its terpenes fraction (ZTE) on HDAC1 and other proteins of the family. A reduction in HDAC1 levels was observed using microglial cells stimulated with bacterial LPS as an *in vitro* model of neuroinflammation. The first aim of this study was to investigate whether the effect of ZOE in the previously studied *in vitro* model of neuroinflammation was that of a pan-HDACi or whether there was selectivity towards specific isoforms. The experiments were carried out on isoforms that were already known
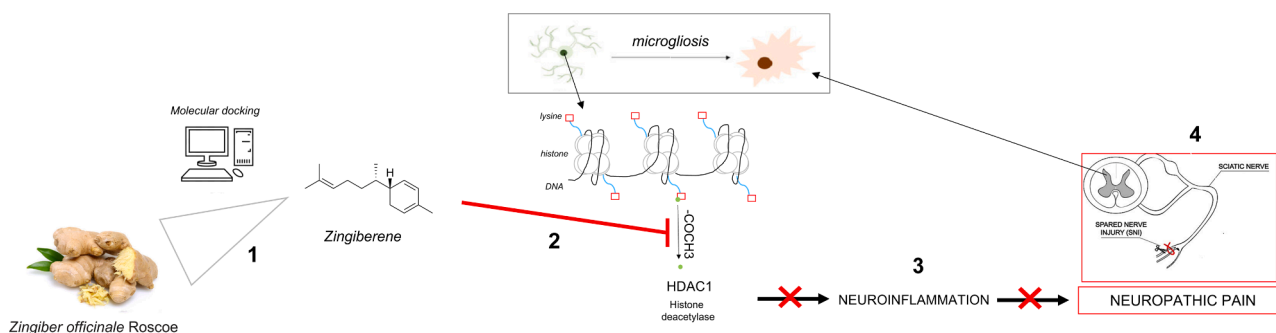
Fig. 5. Summary of the experimental protocol and molecular mechanism of action of ZNG: 1 Molecular docking-based virtual screening of ZTE constituents on HDAC2; 2 ZNG blocked neuroinflammation in BV2 cells by reducing HDAC1 protein expression and activity; 3 The inhibition of HDAC1, which is selectively increased in neuropathic pain, led to the reduction of peripheral neuropathy-related symptoms in mice.

to be expressed in the CNS and at the microglial level, trying to include isoforms belonging to the four different classes (Romanelli et al., 2021). The inflammatory model that we used has already been described in other studies and allowed us to induce the activation of important pathways of the inflammatory process, such as NF-κBp65, in microglia, with the consequent release of inflammatory and oxidative mediators. After an inflammatory stimulus, we observed an increase in HDAC1, 2, 3, 8, and 11 isoforms, while HDAC4, 5, and SIRT1 are not modulated. These results are in line with the findings of Kanna and collaborators (2013), where the maximum gene expression of HDAC4, 5, and SIRT1 was observed with short inflammatory stimuli (4–8 h) while it decreased with time. On the other hand, the increase in the expression of HDAC1, 2, and 3 following stimulations with LPS in microglial cells and their correlation with neuroinflammatory processes is much better documented (Kannan et al., 2013).The anti-inflammatory activities of HDAC8 and HDAC11 at the microglial level also appear to be interesting. A recent study showed that inhibition of HDAC8 reduced neuroinflammation by modulating microglial activation (Lin et al., 2019). ZOE showed a certain selectivity of action, mainly on isoforms belonging to class I (*i.e.*, HDAC1, 2, 8) and class IV (*i.e.*, HDAC11). This selectivity suggests the possible use of ZOE in pathological conditions where specific HDAC isoforms are impaired. Interestingly, the ZTE fraction also showed the same activity on the same isoforms. To confirm the data obtained from *in vitro* test, we used the spared nerve injury (SNI) model, a peripheral neuropathy model induced by trauma. We used this model because in our previous work we observed a potential therapeutical approach of HDAC1 inhibitors for the management of neuropathic pain symptoms through the attenuation of neuroinflammation (Borgonetti et al., 2021a; Romanelli et al., 2021). Particularly, we observed a high value of the co-localization coefficient between HDAC1 and selective microglia markers. Moreover, Datta and collaborators highlighted that deletion of HDAC1 in microglia decreased amyloid load and improved cognitive impairments in a mouse model of Alzheimer's disease, highlighting the strong connection between microglia activity and HDAC1 enzyme (Datta et al., 2018).

In the spinal cord of SNI mice, increased levels of HDAC1, 2, but not HDAC3, 8, and 11 were observed. This effect is consistent with previous studies, reporting that HDAC1 and 2 are the only two isoforms markedly expressed in the SNI model of peripheral neuropathy (Borgonetti et al., 2021b; Ouyang et al., 2019). The selective overexpression of HDAC isoforms appears a specific trait of different neuropathies. An increased expression of HDAC4 was observed in dorsal horn neurons of animals in a spinal nerve ligation (SNL) model (Lin et al., 2015). In addition, ACY-738, a selective HDAC6 inhibitor, can reduce symptoms associated with neuropathic pain in the SNI model, but no information is reported on the expression and localization of this isoform in the spinal cord (Sakloth et al., 2020). The identification of selective HDACi would represent an important step toward a more effective and personalized therapy for neuropathic states. Given the selectivity of action of ZOE and

ZTE on HDAC1 and 2, we performed molecular docking simulations to predict the ZTE constituent with better HDACi activity. ZNG, the main ZTE terpene, was found to have a better binding affinity compared to other constituents. Moreover, its lipophilic features match the hydrophobic nature of HDAC1 binding site, allowing for the establishment of van der Waals contacts with amino acidic residues involved in the binding of other known HDACi. According to molecular docking, ZNG was found to be a non-zinc-binding HDACi, with an IC_{50} of 2.3 μM, which could serve as a scaffold for the design of novel non-zinc-binding analogs with a better safety profile, due to the lack of zinc-binding-mediated off-target effects.

In vivo, the inhibitory effect of ZNG on HDAC1 led to a reduction of the symptoms associated with neuropathic pain, consistently with other HDAC1 inhibitors (Sanna et al., 2017). A previous study showed that HDAC1 inhibition leads to a significant reduction in the activation of NF-κBp65, a well-known marker of microglial activation (Cherng et al., 2014). Also, in this work we observed that ZNG can reduce the expression of HDAC1 and consequently of NF-κBp65 and IL-1β. The antioxidant, anti-inflammatory, and antinociceptive activities of essential oil from ginger has been scarcely investigated. A summary of the experimental protocol and the molecular mechanism of action of ZNG is reported in Fig. 5.

To date, only one other study is available, in which ginger oil (500 mg/kg i.p) led to a significant reduction in acute inflammation produced by carrageenan, dextran, and formalin in mice (Kuttan et al., 2013). The anti-inflammatory and antioxidant activity of ZNG have been reported in cellular models (Li et al., 2021), but this is the first study that demonstrated the activity on HDAC1 expression and the efficacy on controlling SNI-associated neuropathic pain.

Conclusions

Epigenetic enzyme activity is involved in numerous pathophysiological processes with different functions. The overexpression of HDAC1, at the microglial level, in the spinal cord of animals with neuropathy suggest a selective role of this isoform in the progression of this chronic pathology. The majority of the currently available HDAC1 inhibitors are zinc-binding ligands, which could generate numerous side effects due to off-target effects (Romanelli et al., 2021). In this study, we report the selective non-zinc-binding inhibitory activity of ZNG towards class 1 HDACs, which makes this molecule very interesting with possibly fewer side effects and greater selectivity, compared to standard HDACi. ZNG is also already commercially available both as an isolated compound and as a constituent of ginger extracts obtained by supercritical CO2, a method that allows accumulation of this compound in the extraction process, as previously reported (Borgonetti et al., 2020). In conclusion, we found a new non-zinc-dependent inhibitor of HDAC class I, with a therapeutic application in trauma-related NP forms in which microglia-spinal overexpression of HDAC1 occurs.

Declaration of Competing Interest

None.

CRediT authorship contribution statement

Vittoria Borgonetti: Investigation, Methodology, Formal analysis, Writing - original draft. Paolo Governa: Investigation, Methodology, Formal analysis, Writing – original draft. Fabrizio Manetti: Writing - review & editing. Nicoletta Galeotti: Conceptualization, Methodology, Formal analysis, Writing – original draft, Writing - review & editing.

All data were generated in-house, and no paper mill was used. All authors agree to be accountable for all aspects of work ensuring integrity and accuracy.

References

Akone, S.H., Ntie-Kang, F., Stuhldreier, F., Ewonkem, M.B., Noah, A.M., Mouelle, S.E.M., Müller, R., 2020. Natural Products Impacting DNA methyltransferases and histone deacetylases. In Front. Pharmacol. 11 https://doi.org/10.3389/fphar.2020.00992. VolFrontiers Media S.A.

Beshore, D.C., Adam, G.C., Barnard, R.J.O., Burlein, C., Gallicchio, S.N., Holloway, M.K., Krosky, D., Lemaire, W., Myers, R.W., Patel, S., Plotkin, M.A., Powell, D.A., Rada, V., Cox, C.D., Coleman, P.J., Klein, D.J., Wolkenberg, S.E., 2021. Redefining the histone deacetylase inhibitor pharmacophore: high potency with no zinc cofactor interaction. ACS Med. Chem. Lett. 12 (4), 540–547. https://doi.org/10.1021/acsmedchemlett.1c00074.

Block, M.L., Zecca, L., Hong, J.S., 2007. Microglia-mediated neurotoxicity: uncovering the molecular mechanisms. Nature Rev. Neurosci. 8 (1), 57–69. https://doi.org/10.1038/nrn2038. VolIssuepp.

Bondarev, A.D., Attwood, M.M., Jonsson, J., Chubarev, V.N., Tarasov, V.v., Schiöth, H. B., 2021. Recent developments of HDAC inhibitors: emerging indications and novel molecules. Br. J. Clin. Pharmacol. 87 (12), 4577–4597. https://doi.org/10.1111/bcp.14889.

Borgonetti, V., Galeotti, N., 2021a. Combined inhibition of histone deacetylases and BET family proteins as epigenetic therapy for nerve injury-induced neuropathic pain. Pharmacol. Res. 165, 105431 https://doi.org/10.1016/j.phrs.2021.105431.

Borgonetti, V., Galeotti, N., 2021b. Intranasal delivery of an antisense oligonucleotide to the RNA-binding protein HuR relieves nerve injury-induced neuropathic pain. Pain 162 (5), 1500–1510. https://doi.org/10.1097/j.pain.0000000000002154.

Borgonetti, V., Governa, P., Biagi, M., Pellati, F., Galeotti, N., 2020. Zingiber officinale Roscoe rhizome extract alleviates neuropathic pain by inhibiting neuroinflammation in mice. Phytomedicine 78, 153307. https://doi.org/10.1016/j.phymed.2020.153307.

Borgonetti, V., Meacci, E., Pierucci, F., Romanelli, M.N., Galeotti, N., 2022. Dual HDAC/BRD4 inhibitors relieves neuropathic pain by attenuating inflammatory response in microglia after spared nerve injury. Neurotherapeutics 19 (5), 1634–1648. https://doi.org/10.1007/s13311-022-01243-6.

Charan, J., Kantharia, N., 2013. How to calculate sample size in animal studies? J. Pharmacol. Pharmacotherapeutic. 4 (4), 303–306. https://doi.org/10.4103/0976-500X.119726.

Cherng, C.-H., Lee, K.-C., Chien, C.-C., Chou, K.-Y., Cheng, Y.-C., Hsin, S.-T., Lee, S.-O., Shen, C.-H., Tsai, R.-Y., Wong, C.-S., 2014. Baicalin ameliorates neuropathic pain by suppressing HDAC1 expression in the spinal cord of spinal nerve ligation rats. J. Formosan Med. Assoc. 113 (8), 513–520. https://doi.org/10.1016/j.jfma.2013.04.007.

Chuang, D.Y., Simonyi, A., Cui, J., Lubahn, D.B., Gu, Z., Sun, G.Y., 2016. Botanical polyphenols mitigate microglial activation and microglia-induced neurotoxicity: role of cytosolic phospholipase A2. Neuromolecular. Med. 18 (3), 415–425. https://doi.org/10.1007/s12017-016-8419-5.

Curtis, M.J., Alexander, S., Cirino, G., Docherty, J.R., George, C.H., Giembycz, M.A., Hoyer, D., Insel, P.A., Izzo, A.A., Ji, Y., MacEwan, D.J., Sobey, C.G., Stanford, S.C., Teixeira, M.M., Wonnacott, S., Ahluwalia, A., 2018. Experimental design and analysis and their reporting II: updated and simplified guidance for authors and peer reviewers. Br. J. Pharmacol. 175 (7), 987–993. https://doi.org/10.1111/bph.14153.

Datta, M., Staszewski, O., Raschi, E., Frosch, M., Hagemeyer, N., Tay, T.L., Blank, T., Kreutzfeldt, M., Merkler, D., Ziegler-Waldkirch, S., Matthias, P., Meyer-Luehmann, M., Prinz, M., 2018. Histone Deacetylases 1 and 2 regulate microglia function during development, homeostasis, and neurodegeneration in a context-dependent manner. Immunity 48 (3), 514–529. https://doi.org/10.1016/j.immuni.2018.02.016 e6.

du Sert, N.P., Hurst, V., Ahluwalia, A., Alam, S., Avey, M.T., Baker, M., Browne, W.J., Clark, A., Cuthill, I.C., Dirnagl, U., Emerson, M., Garner, P., Holgate, S.T.,

Howells, D.W., Karp, N.A., Lazic, S.E., Lidster, K., MacCallum, C.J., Macleod, M., …, Würbel, H., 2020. The arrive guidelines 2.0: updated guidelines for reporting animal research. PLoS Biol. 18 (7) https://doi.org/10.1371/journal.pbio.3000410.

Ellis, A., Bennett, D.L.H., 2013. Neuroinflammation and the generation of neuropathic pain. Br. J. Anaesth. 111 (1), 26–37. https://doi.org/10.1093/bja/aet128.

Finnerup, N.B., Kuner, R., & Jensen, T.S. (2020). Neuropathic pain 1 neuropathic pain: from mechanisms to treatment.

Forli, S., Huey, R., Pique, M.E., Sanner, M.F., Goodsell, D.S., Olson, A.J., 2016. Computational protein–ligand docking and virtual drug screening with the AutoDock suite. Nat. Protoc. 11 (5), 905–919. https://doi.org/10.1038/nprot.2016.051.

Gao, X., Shen, L., Li, X., Liu, J., 2019. Efficacy and toxicity of histone deacetylase inhibitors in relapsed/refractory multiple myeloma: systematic review and meta analysis of clinical trials. Exp. Ther. Med. https://doi.org/10.3892/etm.2019.7704.

Garden, G.A., 2013. Epigenetics and the modulation of neuroinflammation. Neurotherapeutics 10 (4), 782–788. https://doi.org/10.1007/s13311-013-0207-4.

Hontecillas-Prieto, L., Flores-Campos, R., Silver, A., de Álava, E., Hajji, N., García-Domínguez, D.J., 2020. Synergistic enhancement of cancer therapy using HDAC inhibitors: opportunity for clinical trials. Front. Genet. 11, 1113. https://doi.org/10.3389/fgene.2020.578011.

Kannan, V., Brouwer, N., Hanisch, U.K., Regen, T., Eggen, B.J.L., Boddeke, H.W.G.M., 2013. Histone deacetylase inhibitors suppress immune activation in primary mouse microglia. J. Neurosci. Res. 91 (9), 1133–1142. https://doi.org/10.1002/jnr.23221.

Kuttan, R., Jeena, K., Liju, V.B., 2013. Antioxidant, anti-inflammatory and antinociceptive activities of essential oil from ginger. In Indian J. Physiol. Pharmacol. 57 (1). VolIssue.

Kwon, H.S., & Koh, S.H. (2020). Neuroinflammation in neurodegenerative disorders: the roles of microglia and astrocytes. In Translational Neurodegeneration (Vol. 9, Issue 1). BioMed Central Ltd. doi: 10.1186/s40035-020-00221-2.

Li, J., Thangaiyan, R., Govindasamy, K., Wei, J., 2021. Anti-inflammatory and anti-apoptotic effect of zingiberene on isoproterenol-induced myocardial infarction in experimental animals. Hum. Exp. Toxicol. 40 (6), 915–927. https://doi.org/10.1177/0960327120975131.

Lilley, E., Stanford, S.C., Kendall, D.E., Alexander, S.P.H., Cirino, G., Docherty, J.R., George, C.H., Insel, P.A., Izzo, A.A., Ji, Y., Panettieri, R.A., Sobey, C.G., Stefanska, B., Stephens, G., Teixeira, M., Ahluwalia, A., 2020. ARRIVE 2.0 and the British Journal of Pharmacology: updated guidance for 2020. Br. J. Pharmacol. 177 (16), 3611–3616. https://doi.org/10.1111/bph.15178. VolIssueJohn Wiley and Sons Inc.

Lin, F.-.L., Yen, J.-.L., Kuo, Y.-.C., Kang, J.-.J., Cheng, Y.-.W., Huang, W.-.J., Hsiao, G., 2019. HDAC8 inhibitor WK2-16 therapeutically targets lipopolysaccharide-induced mouse model of neuroinflammation and microglial activation. Int. J. Mol. Sci. 20 (2) https://doi.org/10.3390/ijms20020410.

Lin, T.-.B., Hsieh, M.-.C., Lai, C.-.Y., Cheng, J.-.K., Chau, Y.-.P., Ruan, T., Chen, G.-.D., Peng, H.-.Y., 2015. Modulation of nerve injury–induced HDAC4 cytoplasmic retention contributes to neuropathic pain in rats. Anesthesiology 123 (1), 199–212. https://doi.org/10.1097/ALN.0000000000000663.

Marinelli, S., Basilico, B., Marrone, M.C., Ragozzino, D., 2019. Microglia-neuron crosstalk: signaling mechanism and control of synaptic transmission. In Seminar. Cell Dev. Biol. 94, 138–151. https://doi.org/10.1016/j.semcdb.2019.05.017. VolElsevier Ltd.

Morris, G.M., Huey, R., Lindstrom, W., Sanner, M.F., Belew, R.K., Goodsell, D.S., Olson, A.J., 2009. AutoDock4 and AutoDockTools4: automated docking with selective receptor flexibility. J. Comput. Chem. 30 (16), 2785–2791. https://doi.org/10.1002/jcc.21256.

O'Loughlin, E., Madore, C., Lassmann, H., Butovsky, O., 2018. Microglial phenotypes and functions in multiple sclerosis. Cold Spring Harbor Perspect. Medicine (Baltimore) 8 (2). https://doi.org/10.1101/cshperspect.a028993.

Ouyang, B., Chen, D., Hou, X., Wang, T., Wang, J., Zou, W., Song, Z., Huang, C., Guo, Q., Weng, Y., 2019. Normalizing HDAC2 levels in the spinal cord alleviates thermal and mechanical hyperalgesia after peripheral nerve injury and promotes GAD65 and KCC2 expression. Front. Neurosci. 13, 346. https://doi.org/10.3389/fnins.2019.00346.

Romanelli, M.N., Borgonetti, V., Galeotti, N., 2021. Dual BET/HDAC inhibition to relieve neuropathic pain: recent advances, perspectives, and future opportunities. Pharmacol. Res. 173. https://doi.org/10.1016/j.phrs.2021.105901.

Sakloth, F., Manouras, L., Avrampou, K., Mitsi, V., Serafini, R.A., Pryce, K.D., Cogliani, V., Berton, O., Jarpe, M., Zachariou, V., 2020. HDAC6-selective inhibitors decrease nerve-injury and inflammation-associated mechanical hypersensitivity in mice. Psychopharmacology (Berl.) 237 (7), 2139–2149. https://doi.org/10.1007/s00213-020-05525-9.

Sanna, M.D., Guandalini, L., Romanelli, M.N., Galeotti, N., 2017. The new HDAC1 inhibitor LG325 ameliorates neuropathic pain in a mouse model. Pharmacol. Biochem. Behav. 160, 70–75. https://doi.org/10.1016/j.pbb.2017.08.006.

Subhramanyam, C.S., Wang, C., Hu, Q., Dheen, S.T., 2019. Microglia-mediated neuroinflammation in neurodegenerative diseases. In Seminar. in Cell Dev. Biol. 94, 112–120. https://doi.org/10.1016/j.semcdb.2019.05.004. VolppElsevier Ltd.

Szepesi, Z., Manouchehrian, O., Bachiller, S., & Deierborg, T. (2018). Bidirectional microglia–neuron communication in health and disease. In Frontiers in Cellular Neuroscience (Vol. 12). Media S.A. doi: 10.3389/fncel.2018.00323.

Valente, S., Mai, A., 2014. Small-molecule inhibitors of histone deacetylase for the treatment of cancer and non-cancer diseases: a patent review (2011 –2013). Expert Opin. Ther. Pat. 24 (4), 401–415. https://doi.org/10.1517/13543776.2014.877446.